Mater.Phys.Mech. 4 (2001) 76-80

STM-BASED CHARGE-INJECTION SPECTROSCOPY AT THE ORGANIC/METAL INTERFACE

P. Müller, S.F. Alvarado, L. Rossi and W. Rieß

IBM Research, Zurich Research Laboratory, 8803 Rüschlikon, Switzerland

Received: July 1, 2001

Abstract. We have developed a new method for characterizing the electronic properties of organic thin films and interfaces for electronic device applications. In this scanning tunneling microscope (STM)-based technique, distance versus potential curves are collected at constant tunneling current. Here the STM feedback mechanism causes the tip to penetrate the organic material, allowing the injection barriers at interfaces and charge-transport properties of the organic materials to be determined with nanometer spatial resolution. Moreover, the technique is applicable to organic single and multilayer thin-film samples. Results obtained on thin films of tris(8-hydroxiquinolato)aluminum deposited on Au(111) and Ag(111), and polymorphic copper phthalocyanine deposited on Au(111) substrates will be presented.

1. INTRODUCTION

Current research interest in organic electronic devices is reflected by numerous experimental and theoretical investigations elucidating the underlying physical processes [1–6]. Particular attention is paid to charge-carrier injection from a metal electrode into an organic thin film or from one organic thin film into another, and charge-carrier transport within the organic thin films, all of which are important parameters for device operation.

Recently, scanning tunneling microscopy (STM) imaging has proven to be a powerful tool to investigate these processes locally with resolution on the nanometer scale. Moreover, characterization by STM distance versus potential (*z*–*V*) spectroscopy lets us determine accurate values for the electronic properties. For an overview of STM-based techniques used in this field, see [7].

The barriers for injection of charge carriers from a metal electrode into an organic thin film are determined by the work function of the metal electrode, the highest occupied molecular orbital (HOMO), and the lowest unoccupied molecular orbital (LUMO) of the organic film. Typically, the position of the HOMO level with respect to the Fermi level of the metal electrode is estimated from difference in the ionization potentials (IP) of the materials. This is the so-called common vacuum level (CVL) approximation [8]. The position of the LUMO level is then calculated by adding the optical band gap (E_a) to the HOMO energy. Note, however, that this procedure neglects the influence of interfacial effects such as dipole layers and image forces. Moreover, neither the exciton binding energy (E_b) [9,10] nor the exciton dissociation energy [11] are taken into account. In organic materials, E_b is an important parameter because it exceeds the thermal energy (kT) even at room temperature. The above procedure also disregards the molecular levels of optically forbidden electronic transitions. In this paper we show how STM *z*–*V* spectroscopy can be used to probe directly the injection energies for electrons and holes into polaronic states (E_{p^-} and E_{p^+}, respectively) of the organic material. From these quantities, the single-particle (polaron) energy gap (E_{gsp}) and E_b can be calculated:

Corresponding author: Peter Müller, e-mail: pmu@zurich.ibm.com

© 2001 Advanced Study Center Co. Ltd.

$$E_{gsp} = E_{p^-} - E_{p^+}, \quad (1)$$

$$E_b = E_{gsp} - E_a. \quad (2)$$

In addition, the local mobilities of the electrons (μ^-) and holes (μ^+) of relevance in charge-carrier transport can be qualitatively estimated by comparing the slopes (dz/dV) of the z–V curves, even through all layers of complex organic device structures.

First, we briefly describe the STM z–V spectroscopy technique, and then present representative results obtained on thin films of tris(8-hydroxiquinolato)aluminium (Alq_3) on Au(111) and Ag(111) and of copper-phthalocyanine (CuPc) on Au(111).

2. EXPERIMENTAL

Our experiments were carried out at room temperature under ultrahigh vacuum (UHV) conditions, typically at a base pressure in the 10^{-10} mbar range. A detailed description of the experimental setup can be found in Ref. [12]. To acquire the STM z–V spectra, platinum-iridium tips were used. The organic thin-film samples were prepared in-situ in a UHV chamber [12] by thermal evaporation on atomically flat Au(111) and Ag(111) substrates at room temperature [7]. The as-grown Alq_3 thin films on Au(111) and Ag(111) and CuPc thin films on Au(111) typically are 3 to 5 nm thick. For further details regarding sample preparation and the morphologies observed using STM, the reader is referred to [7, 13–15].

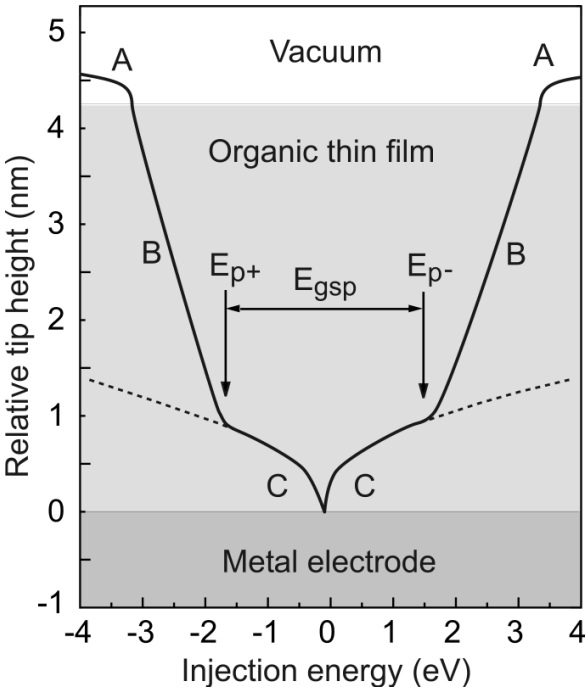

Fig. 1. Schematic of a STM z–V injection spectrum (solid curve). E_{p^-} and E_{p^+} are the thresholds of the charge-injection energies for electrons and holes into polaronic states, respectively, and E_{gsp} is the single-particle energy gap. The dashed curves represent typical STM tip displacements observed at a clean metal surface. Phases A to C are discussed in the text.

3. STM z–V SPECTROSCOPY

In contrast to conventional STM current–voltage (I–V) spectroscopy [16–18], which has to open the feedback loop during operation and measures the energy dependence of the density of states (DOS) [19], STM z–V spectroscopy probes the DOS via the voltage-dependent tip displacement at constant tunneling current. Fig. 1 shows a schematic z–V spectrum of a thin film, which typically consists of three consecutive phases, indicated by A, B and C.

Phase A: Under normal conditions, the tunneling resistance (R_t) is much larger than the resistance of the organic layers (R_{org}). Thus R_t is given by

$$R_t = \frac{V_t}{I_t}, \quad (3)$$

where V_t is the tunneling bias voltage and I_t the tunneling current. Charge-carrier injection takes place through the vacuum barrier into the organic material, see Fig. 2(a). This means that the applied bias voltage V_t drops completely at the tunneling barrier, and the charge-injection energy, E_t, can be tuned by adjusting polarity and magnitude of V_t:

$$E_t = V_t \cdot e, \quad (4)$$

where e is the single electron charge. Reducing the bias voltage under constant-current conditions forces the tip into close proximity and finally into direct physical contact with the organic thin film.

Phase B: When this contact mode has been attained, the Fermi level of the tip typically will be at an energy level within the forbidden energy gap of the organic material. The high electrical field across the organic layer leads to band bending and the formation of a Schottky-like diode, see Fig. 2(b). The gradient of the electrical field strongly depends on the curvature of the injecting electrodes. Thus, the highest electrical field drop appears at the STM tip apex, which, under ideal conditions, will be the predominant site for charge-carrier injection into the

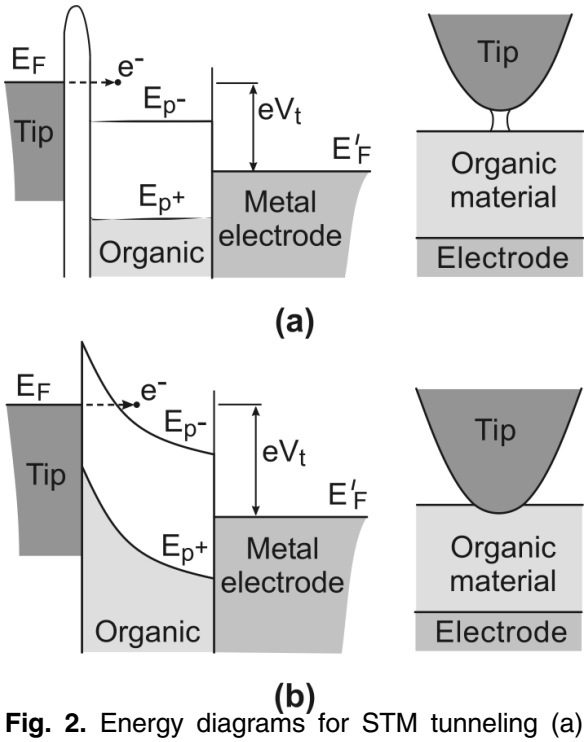

Fig. 2. Energy diagrams for STM tunneling (a) through a vacuum barrier into the organic thin film and (b) through a Schottky-like barrier with the tip in contact. In both cases, a negative tip bias (V_t < 0) relative to the Fermi level of the metal electrode is shown.

organic thin film, see Fig. 2(b). For example, with a typical STM tip apex radius $R \cong 50$ nm, one can obtain continuous injection current densities in the range of j = 10 to 10^4 A/cm^2 at a V_t of a few volts, which is orders of magnitude higher than current densities at the planar interface between the organic material and the metal electrode shown in Fig. 2. Note that the injection process can either be thermionic emission or tunneling [20,21]. A more detailed description of tip geometries and its local current densities can be found in [7,22,23].

Phase C: Injection of charge carriers into the organic material is possible until $|V_t|$ is reduced to the value at which the Fermi level of the tip enters the forbidden energy gap at the interface with the metal electrode. The point at which this transition occurs determines the position of the lowest electron polaron state (E_{p^-}) for an applied V_t < 0 or the highest polaron state (E_{p^+}) for V_t > 0 (see arrows in Fig. 1, tip polarity with respect to the Fermi level of the substrate). In this phase, a characteristic logarithmic *z*–*V* curve is observed when either tunneling directly into the metal electrode or nonresonantly through a monomolecular organic layer in contact with the electrode.

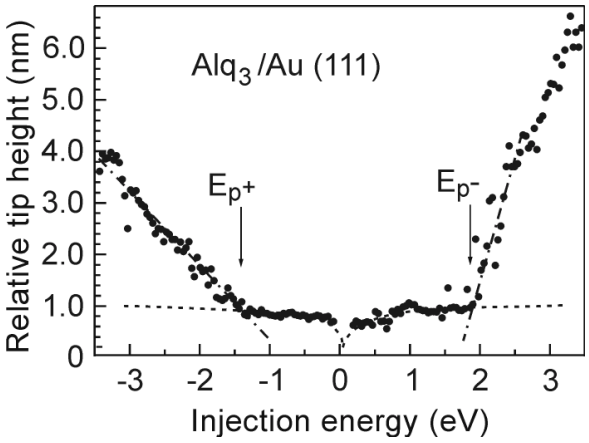

Fig. 3. Typical STM z–V curve of an Alq_3 thin film on Au(111). The injection barriers for electrons (E_{p^-}) and holes (E_{p^+}) into organic states are marked by arrows. The dashed curve is the tip displacement, measured for a clean Au(111) surface. The *dz*/*dV* slope of the dash-dotted lines is a measure for the mobilities of the electron and hole polarons. The much steeper slope for E_{p^-} is proof that Alq_3 is a good electron-transport material.

3.1. Measurements on Alq_3

STM images taken at different positions and on various samples reveal that for very thin films, a few nanometers thick, the surface exhibits unaligned nano-crystallites [7,24]. Fig. 3 shows a typical *z*–*V* spectroscopy curve collected on Alq_3 on Au(111). For this system we obtained E_{p^-}=1.15 ± 0.18 meV and E_{p^+}=-1.81 ± 0.25 meV relative to the Au(111) Fermi level. The slope *dz*/*dV* of the *z*–*V* curve acquired with negative tip bias is much steeper than that of the curve taken with positive tip bias. This confirms that Alq_3 preferentially transports electrons and that $\mu^- >> \mu^+$ [7,25].

The injection barrier determined from *z*–*V* spectroscopy for electrons into Au(111) is ≅ 200 meV higher than into Ag(111). However, the difference of the work functions of Au(111) and Ag(111) is approx. 600 meV [26], thus revealing a significant deviation from the CVL approximation. This difference could possibly be explained by image forces or dipole layers at the organic/metal interface (see [1]).

A statistical analysis of measurements taken on Au(111) and Ag(111) yields two peaks for the E_{p^-} values. These two values for E_{p^-}, $E_{p^-} \cong 1.15$ and ≅1.7 eV, indicate that two different types of surface configurations between the organic material and the metal electrode exist. The E_{gsp} values for the two

configurations are 2.96 and 3.04 eV. Possible explanations for this behavior are various morphologies of the Alq_3 thin film [24] or different electronic properties of the two existing Alq_3 isomers [7,13,27].

3.2. Measurements on CuPc

STM images of as-grown CuPc on Au(111) thin films are featureless, an indication that these films are completely disordered. However, after annealing for 1 h at 600K, the organic thin film reconstructed into various polymorphic crystallites. These crystallites are about 30–40 monolayers thick, several 100 nm in diameter, and strongly resemble the bulk (α) and (β) phases [14,15].

On the disordered phase, we obtained E_{p^-}= 550 ± 150 meV and E_{p^+}=-550 ± 150 meV, relative to the Au(111) metal electrode, which yield E_{gsp} = 1.1 ± 0.2 eV. For this special case, we also measured E_{gsp} directly by ramping V_t from positive to negative. This yields E_{gsp} = 950 ±100 meV.

For the β_2 phase [14], we find E_{p^-}= 100 ± 50 meV, E_{p^+}=-200 ± 50 meV, and E_{gsp} = 300 ± 70 meV. The slopes of these *z–V* curves are approximately two orders of magnitude steeper than that of the disordered phase, indicating much higher values of μ^- and μ^+ for the β_2 phase. For polymorphic CuPc, Eq. (1) leads to an actual E_{gsp} that is much smaller than E_a >> 1.6 to 1.7 eV [28,29], suggesting that charge carriers are injected into non-optically active states, see [14,15].

4. CONCLUSIONS

STM *z–V* spectroscopy is a powerful method for characterizing the electronic properties of organic/metal and organic/organic interfaces. An important capability of this technique is that it allows the direct measurement of the molecular level alignments of the occupied and empty states. This means that it is even possible to probe charge-carrier injection into electronic states that are optically forbidden.

From the injection barriers (E_{p^-} and E_{p^+}), the single-particle energy gap (E_{gsp}) and, together with the optical band gap (E_a), the exciton binding energy (E_b) can be calculated. Furthermore, a qualitative measure of the local mobility of the electrons and holes can be derived from the slope *dz*/*dV* of the *z–V* curves.

Because the injection barriers for electron- and hole-charge carriers obtained from STM *z–V* spectroscopy are quantitatively very accurate, they form an ideal basis for future theoretical investigations and device modeling.

ACKNOWLEDGMENTS

We thank H. Riel and T. Beierlein for helpful discussions. This work was performed within the Training and Mobility of Researchers Network EUROLED, and supported by grants from the Swiss Federal Office for Education and Science and by the European Commission (FMRX-CT97-0106).

REFERENCES

[1] H. Ishii, K. Sugiyama, E. Ito and K. Seki // *Adv. Mater.* **11** (1999) 605.
[2] A. Rajagopal, C.I. Wu and A. Kahn // *J. Appl. Phys.* **83** (1998) 2649.
[3] S.T. Lee, X.Y. Hou, M.G. Mason and C.W. Tang // *Appl. Phys. Lett.* **72** (1998) 1593.
[4] W. Brütting, S. Berleb and A. Mückel // *Org. Electron.* **2** (2001) 1.
[5] H. Baessler // *phys. status solidi b* **175** (1993) 15.
[6] N. Graham, R. Friend, in: *Solid State Physics, Advances in Research and Applications, Vol. 49*, ed. by H. Ehrenreich and F. Spaepen (Academic Press, San Diego, CA, 1995) p. 2.
[7] S.F. Alvarado, L. Rossi, P. Müller and P.F. Seidler // *IBM J. Res. Develop.* **45** (2001) 89.
[8] W. Schottky // *Z. Phys.* **118** (1942) 539.
[9] E.M. Conwell // *Synth. Met.* **83** (1996) 101.
[10] I.H. Campbell, T.W. Hagler, D.L. Smith and J.P. Ferraris // *Phys. Rev. Lett.* **76** (1996) 1900.
[11] D. Woehrle, L. Kreienhoop and D. Schlettwein, in: *Phthalocyanines Properties and Applications*, ed. by C.C. Leznoff and A.B.P. Lever, Vol. 4, (VCH Publishers, New York, 1996) p. 223.
[12] S.F. Alvarado, W. Rieß, M. Jandke and P. Strohriegl // *Org. Electron.* **2** (2001) 75.
[13] S.F. Alvarado, L. Libioulle and P.F. Seidler // *Synth. Met.* **91** (1997) 69.
[14] S.F. Alvarado, L. Rossi, P. Müller and W. Rieß // *Synth. Met.* **122** (2001) 73.
[15] L. Rossi, P. Müller, S.F. Alvarado and W. Rieß, *Charge-carrier injection into polymorphic forms of CuPc: A scanning tunneling microscopy study* (in preparation).
[16] N.D. Lang // *Phys. Rev. Lett.* **58**, 45 (1987).
[17] S. De Cheveigne, J. Klein and A. Leger, in: *Tunneling Spectroscopy*, ed. by P.K. Hansma (Plenum Press, New York, 1982) p. 109.
[18] R. Wiesendanger, *Scanning Probe Microscopy and Spectroscopy, Methods and Applications* (Cambridge University Press, Cambridge, UK, 1994).

[19] R. Feenstra // *Phys. Rev. B* **50** (1994) 4561.
[20] E.M. Conwell and E.W. Wu // *Appl. Phys. Lett.* **70** (1997) 1867.
[21] M.N. Bussac, D. Michoud and L. Zuppiroli // *Phys. Rev. Lett.* **81** (1998) 1678.
[22] M.A. Lampert and P. Mark, *Current Injection in Solids*, ed. by H.G. Booker and N. DeClaris (Academic Press, New York, 1970).
[23] M.K. Miller, A. Cerezo, M.G. Hetherington and G.D.W. Smith, in: *Atom Probe Field Ion Microscopy* (Oxford University Press, Oxford, UK, 1996), p. 41.
[24] M. Birkmann, G. Gadret, M. Muccini, C. Taliani, N. Masciocchi and A. Sironi // *J. Am. Chem. Soc.* **122** (2000) 5147.
[25] T. Tsutsui, H. Tokuhisa and M. Era, in: *Polymer Photonic Devices,* ed. by B. Kippelen and D.D. Bradley, Proc. SPIE, Vol. 3281 (SPIE, Bellingham, WA, 1998) p. 230.
[26] H.B. Michelson // *J. Appl. Phys.* **48** (1997) 4729.
[27] A. Curioni and W. Andreoni // *IBM J. Res. Develop.* **45** (2001) 101.
[28] E.A. Lucia and F.D. Verderame // *J. Chem. Phys.* **48** (1968) 2674.
[29] B.R. Hollebone and M.J. Stillman // *J. Chem. Soc. Faraday Trans. II* **74** (1978) 2107.